Mon. Not. R. Astron. Soc. **000**, 000–000 (0000) Printed 1 February 2008 (MN LaTeX style file v1.4)

The Cosmological Dependence of Galactic Specific Angular Momenta

Vincent Eke, George Efstathiou & Lisa Wright
Institute of Astronomy, Madingley Road, Cambridge CB3 OHA.

1 February 2008

ABSTRACT

Hydrodynamical simulations of galaxy formation in spatially flat Cold Dark Matter (CDM) cosmologies with and without a cosmological constant (Λ) are described. A simple star formation algorithm is employed and radiative cooling is allowed only after redshift $z = 1$ so that enough hot gas is available to form large, rapidly rotating stellar discs if angular momentum is approximately conserved during collapse. The specific angular momenta of the final galaxies are found to be sensitive to the assumed background cosmology. This dependence arises from the different angular momenta contained in the haloes at the epoch when the gas begins to collapse and the inhomogeneity of the subsequent halo evolution. In the Λ-dominated cosmology, the ratio of stellar specific angular momentum to that of the dark matter halo (measured at the virial radius) has a median value of ~ 0.24 at $z = 0$. The corresponding quantity for the $\Lambda = 0$ cosmology is over 3 times lower. It is concluded that the observed frequency and angular momenta of disc galaxies pose significant problems for spatially flat CDM models with $\Lambda = 0$ but may be consistent with a Λ-dominated CDM universe.

Key words: galaxies: formation – galaxies: evolution – galaxies: spiral – cosmology: theory – dark matter

1 INTRODUCTION

Smoothed Particle Hydrodynamical (SPH) simulations of galaxy formation in Cold Dark Matter (CDM) dominated universes have repeatedly failed to create Milky Way-type extended discs (Navarro & Benz 1991; Katz 1992; Navarro, Frenk & White 1995; Steinmetz & Muller 1995; Navarro & Steinmetz 1997; Weil, Eke & Efstathiou 1998, hereafter WEE98). Gas is found to cool very effectively at high redshifts into the centres of haloes before gravitational torques from surrounding perturbations can supply it with sufficient angular momentum. Furthermore the lumpy nature of the subsequent halo evolution leads to an outward transfer of angular momentum, compounding the problem. Navarro & Steinmetz (1997) showed that including a photoionizing background to suppress the early cooling of gas, worsened the problem by preferentially decreasing the amount of higher angular momentum gas accreted at late epochs.

Almost all analytic and semi-analytic models of galaxy formation assume that angular momentum is conserved during disc formation (Mestel 1963; Fall & Efstathiou 1980; Gunn 1982; van der Kruit 1987; Cole et al. 1994; Dalcanton, Spergel & Summers 1997; Mo, Mao & White 1998), in marked contrast to what is found in numerical simulations. It is interesting to note that Cole et al. (1994) actually find that their predicted Tully-Fisher relation has galaxies spinning 60 per cent too rapidly at fixed luminosity, or alternatively being underluminous at fixed circular velocity. Evidently, the degree to which angular momentum is conserved during galaxy formation is of vital importance in developing realistic theoretical models for comparison with observations.

Given that high angular momentum gas is required to produce a rapidly spinning large stellar disc, and recognising that the collapse of gas to form such a disc will, if anything, transfer angular momentum to the halo, it is apparent that a significant reservoir of hot gas must be maintained in the galactic halo at least until the epoch at which the halo specific angular momentum has grown to match that of real galaxies. As discussed above, numerical simulations have generally failed to do this. Navarro & Benz (1991), WEE98 and others, have suggested that the inclusion of a more effective feedback mechanism, in particular, energy injection from supernovae (see *e.g.* Larson 1974, Dekel and Silk 1986) is the most likely solution to this problem. To illustrate the importance of feedback, WEE98 performed several SPH simulations of haloes selected from CDM initial conditions in an $\Omega = 1$, $\Lambda = 0$, universe with radiative cooling suppressed until a redshift $z = 1$. They did indeed find that suppressing the collapse of gas until late epochs had a dramatic effect on the specific angular momentum of the final galaxies. However, only two out of five carefully selected haloes produced

objects with comparable angular momenta to those of real disc galaxies. This suggests that even with an extreme feedback prescription, there may be a problem explaining the frequency and angular momenta of disc galaxies in a critical density CDM universe with $\Lambda = 0$.

This problem is investigated in more detail in this letter and the sensitivity of the specific angular momenta of the final objects to the assumed background cosmology is tested. The same simplified feedback prescription of WEE98 is adopted, *i.e.* radiative cooling is suppressed until $z = 1$, and applied to a total of 60 SPH simulations for two spatially flat CDM universes, one with $\Omega_m = 1$ and $\Lambda = 0$ and the other with $\Omega_m = 0.3$ and $\Omega_\Lambda = 0.7$. Section 2 contains details of the two cosmological models, the initial conditions of the SPH simulations and the simulations themselves. The results are presented in Section 3 and discussed in Section 4.

2 SIMULATION DETAILS

2.1 Model parameters

The two spatially flat CDM cosmological models that are investigated have scale invariant initial fluctuations and a post-recombination power spectrum given by the parametrisation of Efstathiou, Bond & White (1992) with a shape parameter $\Gamma = 0.2$. One model, referred to as τCDM (following the nomenclature of Thomas et al. 1998) has a matter density parameter $\Omega_m = 1$ and zero cosmological constant. The other model, ΛCDM has $\Omega_m = 0.3$ and a cosmological constant contributing $\Omega_\Lambda = 0.7$ to the density parameter; the parameters for this model are close to those favoured by anisotropies in the cosmic microwave background radiation and the distances of Type Ia supernovae (see *e.g.* Efstathiou et al. 1999). The amplitude of the mass fluctuations has been normalised to reproduce the present day abundance of galaxy clusters, thus the linear theory *rms* mass fluctuations in spheres of radius $8h^{-1}$ Mpc are $\sigma_8 = 0.52$ and 0.90 for the τCDM and ΛCDM models respectively (Eke et al. 1996). In both models the Hubble constant is set to $h = 0.65^\star$, giving an age for the τCDM universe of 10.0 Gyr and 14.5 Gyr for ΛCDM. The baryonic contribution to the critical density is set to $\Omega_{\rm b} = 0.06$ in both models, consistent with the predictions of primordial nucleosynthesis and the deuterium abundance measurements reported by Burles & Tytler (1998).

2.2 Dark matter simulations

To create initial conditions for the SPH simulations, a dark matter only calculation was performed for each cosmology using the AP^{3}M code of Couchman (1991). For each cosmology, a 32.5 h^{-1} Mpc cube containing 128^3 particles was evolved from $z = 24$ to the present employing 2000 timesteps of equal size in expansion factor. The effective Plummer gravitational force softening was fixed in comoving coordinates at 7 kpc. Identical random phases were used in both simulations so that the same haloes in both cosmologies could be simulated at higher resolution with the SPH code.

* h is defined such that $H_0 = 100h$ km s^{-1}Mpc^{-1}.

2.3 Halo selection

The spherical overdensity group-finding algorithm (Lacey & Cole 1994) was applied to the final outputs of the dark matter simulations to locate virialised haloes, with the virial radius defined by the spherical collapse model. A subset of these were chosen for resimulation with the SPH code. To qualify for resimulation, a halo had to be at least $1h^{-1}$ Mpc from any other containing at least 100 particles at $z = 0$. This constraint was applied so that the effort in the resimulation was concentrated on the central object rather than a more massive companion. It effectively biases against haloes in dense environments and can be loosely thought of as selecting a sample of field galaxies. Twenty haloes that could clearly be identified as the same object in both τCDM and ΛCDM simulations with circular velocities in the range $170 < v_{\rm c}/$ km s^{-1} < 250 in the τCDM run were selected for resimulation (referred to as 'common' haloes hereafter). As the corresponding ΛCDM haloes had systematically lower circular velocities (by about 30 per cent), 5 additional larger ΛCDM and 15 smaller τCDM haloes were also chosen to increase the overlap in circular velocity between the two models. WEE98 adopted similar algorithms to select haloes, but also imposed an additional constraint that the haloes should not have merged with a comparable mass system between $z = 1$ and $z = 0$. This criterion was imposed to bias against haloes that suffered a major merger at late times and hence to select haloes more favourable to the formation of disc systems. No such criterion was applied in generating initial conditions for the simulations described in this paper.

2.4 SPH Simulations

The procedure for creating high resolution initial conditions for resimulation is as described by WEE98. Briefly, this involved tracing back to the initial redshift all dark matter particles within 400 kpc of the selected halo centres at $z = 0$. Extra particles were placed in a 'high resolution' cube containing the region of interest (and including the short wavelength fluctuations associated with this improved resolution) and more massive particles were added to sample the distant density field. 34^3 dark matter and 34^3 gas particles (initially at identical positions to the dark particles) were used in the central cube, while the outer regions were represented by ~ 5000 particles with radially increasing masses. The sizes of the high resolution cubes were typically about $3.2h^{-1}$ Mpc and $4.0h^{-1}$ Mpc for τCDM and ΛCDM simulations, yielding gas particle masses of $\sim 2 \times 10^7 {\rm M}_\odot$ and $4 \times 10^7 {\rm M}_\odot$ respectively. Higher resolution runs with 2×43^3 particles were also performed for some of the τCDM haloes that produced inadequately resolved stellar discs.

The evolution of the simulation was performed using the GRAPESPH code outlined in WEE98 and 5 GRAPE$-3A$ boards (Sugimoto et al. 1990) connected to a Sun Ultra-2 workstation. The Plummer gravitational force softening for gas and star particles was 0.8 kpc and the dark matter had softenings of 4.1 kpc and 2.7 kpc for τCDM and ΛCDM respectively. Up to 40000 timesteps for τCDM and 60000 for ΛCDM runs were used to evolve the particles from $z = 24$ to $z = 0$. Typical run times were 2 days for each τCDM simulation and $3 - 4$ days for a ΛCDM simulation. Radiative

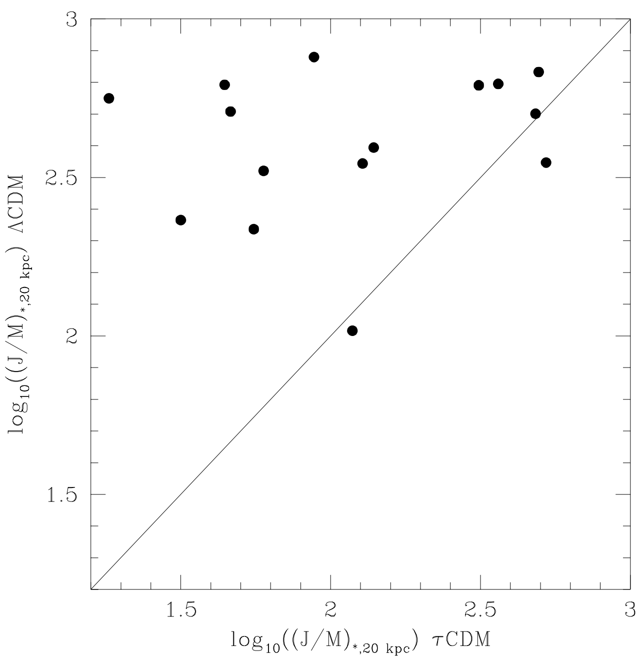

Figure 1. The correlation of the stellar specific angular momenta for the τCDM and ΛCDM SPH simulations of 'common' haloes (*i.e.* haloes clearly identified as the same object in both cosmologies, see Section 2.3). The stellar specific angular momentum is computed for stars within 20kpc of the stellar centre. Results are shown only for systems that contain more than 1000 stars.

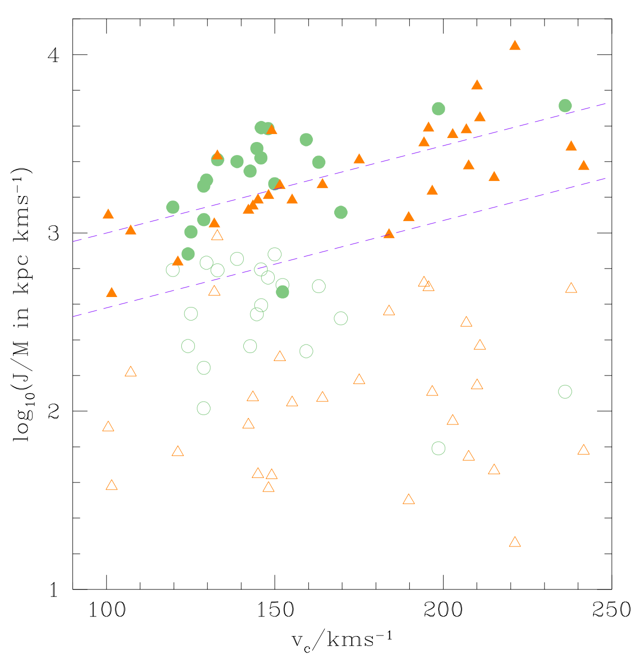

Figure 2. Specific angular momenta of the dark matter haloes, determined at the virial radius, and the stellar components, at 20 kpc. τCDM haloes and stellar components are represented by filled and open triangles, while the corresponding ΛCDM variables are shown with filled and open circles. The dotted lines delineate the approximate 90 percentile range of specific angular momenta of observed disc systems derived from the sample analysed by WEE98, converted to a Hubble constant of $h = 0.65$ and assuming that the discs are perfectly cold and have flat rotation curves.

cooling was switched on at $z = 1$ in all cases to model feedback crudely, as described by WEE98. Each gas particle that remained in a collapsing region with $\rho > 7 \times 10^{-23}$ kg m^{-3} (see Navarro & White 1993, WEE98) for a local dynamical time was converted to a star particle.

3 RESULTS

The same number of particles is used in the high resolution regions even though these differ in volume from run-to-run. The numerical resolution of the SPH simulations is therefore variable and correlated with the mass of the halo. Navarro & Steinmetz (1997) discussed in detail the outward transport of angular momentum when the SPH artificial viscosity acts on a poorly resolved gaseous disc. As a result of the star formation algorithm adopted here, the gaseous discs do not monotonically increase their masses, and thus the effect of this viscous transport is probably increasing as the simulations approach $z = 0$ and the accretion rate diminishes. However, by analysing the conservation of angular momentum as a function of the number of star particles within 20 kpc of the halo centre, it was found that only systems with less than ~ 1000 stars showed any significant trend of increasing angular momentum with increasing mass resolution. Consequently, results will only be given for simulations that had at least 1000 stars in the central object at $z = 0$.

Figure 1 shows an object by object comparison of the stellar specific angular momenta for the common haloes in the two sets of simulations. The stellar angular momentum is measured for the central galaxy-like object within 20 kpc of its centre. There is essentially no correlation between the two quantities. However, the galaxies in the ΛCDM simulations tend to have significantly more angular momentum than their τCDM counterparts. The reasons for this difference will be discussed in more detail below.

Figure 2 shows the absolute specific angular momenta of all the dark matter haloes (i.e. not just the common haloes), measured at the virial radius, and their largest stellar occupants, as a function of halo circular velocity. The dashed lines in Figure 2 show the ranges of specific angular momenta of real disc galaxies[†] (see figure 1 of WEE98). While the haloes in both cosmologies occupy a similar locus (for $120 < v_c/\mathrm{km\,s^{-1}} < 180$, the ΛCDM haloes are only ~ 50 per cent higher than those for τCDM), the τCDM stellar objects are at systematically much lower values than those from the ΛCDM simulations. For both sets of simulations the fraction of halo specific angular momentum retained in the stellar objects decreases with increasing circular speed. Thus in comparing the two cosmologies, attention will be restricted to haloes with circular speeds in the same

[†] The observed specific angular momenta are calculated assuming flat rotation curves of amplitude v_c. For dark haloes with the Navarro, Frenk and White (1996) profile, the disc rotation velocity may exceed the halo circular speed at the virial radius by as much as 30–40 %, depending on the concentration of the stellar disc. This difference is neglected in this paper.

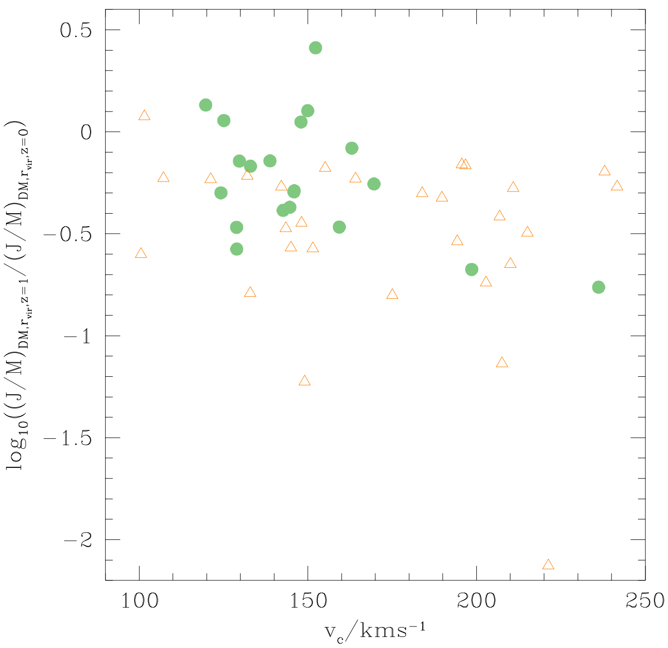

Figure 3. The ratio of $z = 1$ to $z = 0$ halo specific angular momenta for τCDM (open triangles) and ΛCDM (filled circles) simulations plotted as a function of circular velocity.

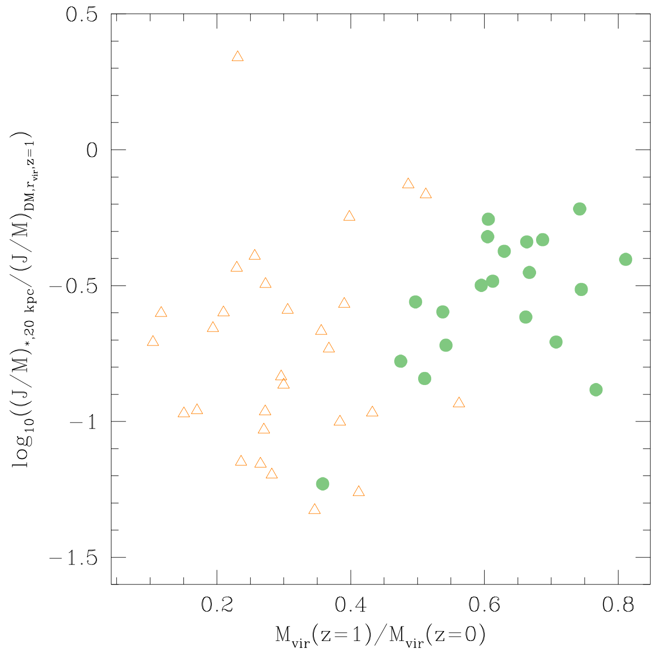

Figure 4. The correlation between the ratio of halo virial mass at $z = 1$ to $z = 0$ and the conserved specific angular momentum. τCDM results are shown with open triangles and ΛCDM with filled circles.

range, $120 < v_c/\mathrm{km\,s^{-1}} < 180$. For the 12 τCDM and 17 ΛCDM haloes that this range includes, the median ratios of stellar to halo specific angular momenta at $z = 0$ are 0.07 and 0.24 respectively.

One reason for this difference is that although haloes in the τCDM and ΛCDM models with the same circular speed have similar angular momenta at $z = 0$, the angular momentum growth depends on the background cosmology. As a consequence of the continual evolution of structure in the τCDM model, haloes acquire relatively more angular momentum since $z = 1$ than haloes in the ΛCDM model. This is illustrated in Figure 3. Since typically half of the stars are formed by $z = 0.4$ in the τCDM simulations and by $z = 0.6$ for ΛCDM, it is more appropriate to compare final stellar angular momenta with those of the parent haloes at $z = 1$ when disc formation begins. For haloes with circular speeds in the range $120 < v_c/\mathrm{km\,s^{-1}} < 180$ the median ratios of stellar to halo specific angular momenta at $z = 1$, are 0.17 and 0.32 for τCDM and ΛCDM respectively. Thus a major reason for the differences in final stellar angular momenta in the two cosmologies is that τCDM haloes have lower angular momenta at $z \sim 1$ compared with ΛCDM haloes of the same circular speed.

The other main cause of the difference in stellar angular momenta in the two cosmologies stems from the more inhomogeneous evolution at $z < 1$ suffered by τCDM haloes. As a consequence of the higher frequency of merger events in the τCDM cosmology, the accretion at late times of high angular momentum gas from the outer parts of the halo is disrupted. Either the gas is gravitationally shocked and remains extended, or its angular momentum is transported to larger radii by torques from the anisotropic halo. Figure 4 shows how the fraction of conserved specific angular momentum varies with the halo growth, parametrised by the ratio of halo virial masses at $z = 1$ to $z = 0$. It is clear that the ΛCDM haloes accrete significantly less mass than those evolving in the τCDM model. Galaxies forming in the ΛCDM cosmology experience fewer merger events and conserve a greater fraction of their angular momentum.

4 CONCLUSIONS

The aim of this work has been to investigate how the background cosmological model affects the efficiency with which angular momentum is conserved during galaxy formation. The large set of simulations described here shows that the specific angular momenta of galaxies with halo circular speeds in the range 120–180 $\mathrm{km\,s^{-1}}$ forming in a ΛCDM universe are typically $3 - 4$ times higher than those in a τCDM universe. This large difference arises from the more turbulent merger histories of the τCDM haloes and from their lower specific angular momenta.

The median specific angular momentum for observed disc galaxies (see the dashed lines in Figure 2 and figure 1 of WEE98) is, nevertheless, about 2.5 times as large as that of the ΛCDM galaxies simulated here, and an order of magnitude above the τCDM galaxies. This discrepancy for the τCDM model is extremely large, confirming the suspicion of WEE98 that the observed frequency of disc galaxies is difficult to reproduce in a spatially flat CDM model with $\Lambda = 0$. Allowing cooling at higher redshift would exacerbate this problem (see WEE98), and it seems unlikely that a more realistic feedback process could resolve this discrepancy.

In both cosmologies there is a strong trend for galaxies with high circular speeds to lose more angular momen-

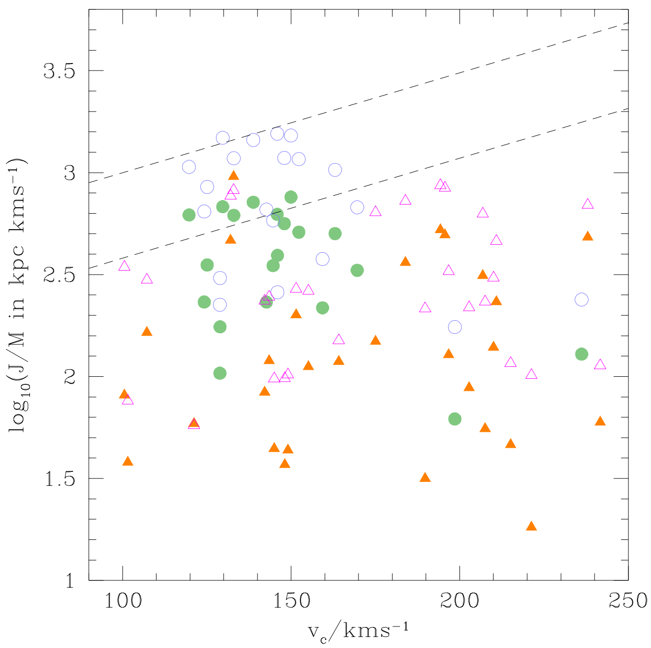

Figure 5. The stellar specific angular momenta for τCDM and ΛCDM galaxies are shown with filled triangles and circles, as a function of circular velocity. The corresponding open symbols represent the results obtained when stars within a central sphere of 3 kpc are excluded from the calculation. Dashed lines show the range of specific angular momenta of real disc galaxies as plotted in Figure 2.

tum, suggesting that it is difficult to form large disc galaxies within haloes with circular speeds of $\gtrsim 200\mathrm{km\,s}^{-1}$ at the virial radius. This is qualitatively consistent with the observed lack of spiral discs with high circular speeds.

Most of the simulated galaxies in the ΛCDM cosmology lie below the observed range of specific angular momenta for real disc systems, though the magnitude of the discrepancy is much lower than in the τCDM cosmology. This may not be an insurmountable problem for the ΛCDM model. The observational range plotted in Figure 2 is computed from the specific angular momenta of only the disc components, whereas the specific angular momenta of the simulated galaxies have been calculated using the entire stellar system. In a more realistic scenario, the low angular momentum gas might be expected to give rise to a bulge-type stellar component in addition to providing the feedback energy to maintain the reservoir of hot, extended and high angular momentum gas at large redshift. Figure 5 shows that removing all stars within a 3 kpc sphere of the centres of the final stellar objects can bring the ΛCDM galaxies with circular speeds $\lesssim 180\mathrm{km\,s}^{-1}$ into agreement with the observations. The choice of 3 kpc is arbitrary and has been adopted merely to illustrate the importance of correctly distinguishing between an inner bulge and an extended disc before comparing simulations with observations. To do this more accurately will require a more realistic feedback prescription and much larger numerical simulations in which bulge and disc components can be distinguished kinematically. Until such simulations are performed, it is unclear whether the ΛCDM model can account for the observed frequency of disc galaxies. However, galaxies forming in a τCDM-like universe experience a severe 'angular momentum catastrophe' and this seems to be a fundamental problem for such a model.

ACKNOWLEDGMENTS

VE, GE and LW acknowledge the support of a PPARC postdoctoral fellowship, senior research fellowship and research studentship respectively. We thank the Institute of Astronomy for providing funds towards the purchase of the GRAPE boards.

REFERENCES

Burles S., Tytler D., 1998, ApJ, 507, 732
Cole S., Aragon-Salamanca A., Frenk C.S., Navarro J.F., Zepf S., 1994, MNRAS, 271, 781
Couchman H.M.P., 1991, ApJ, 429, L23
Dalcanton J.J., Spergel S.N., Summers F.J., 1997, ApJ, 482, 669
Dekel A., Silk J., 1986, ApJ., 303, 39
Efstathiou G., Bond J.R., White S.D.M., 1992, MNRAS, 258, L1
Efstathiou G., Bridle S.L., Lasenby A.N., Hobson M.P., Ellis R., 1999, MNRAS, 303, L47.
Eke V.R., Cole S., Frenk C.S., 1996, MNRAS, 282, 263
Fall S.M., Efstathiou G., 1980, MNRAS, 193, 189
Gunn J.E., 1982, in Astrophysical Cosmology, ed. H.A. Bruck, G. Coyne and M.S. Longair, (Vatican Pontificia Acadamia Scientiarum), 191
Katz N., 1992, ApJ, 391, 502
Kauffmann G., White S.D.M., Guiderdoni B., 1993, MNRAS, 264, 201
Lacey C., Cole S., 1994, MNRAS, 271, 676
Larson R.B., 1974, MNRAS, 169, 229
Mestel L., 1963, MNRAS, 126, 553
Mo H.J., Mao S., White S.D.M., 1998, MNRAS, 295, 319
Navarro J.F., Benz W., 1991, ApJ, 380, 320
Navarro J.F., White S.D.M., 1993, MNRAS, 265, 271
Navarro J.F., Frenk C.S., White S.D.M., 1995, MNRAS, 275, 56
Navarro J.F., Frenk C.S., White S.D.M., 1996, ApJ, 462, 536
Navarro J.F., Steinmetz M., 1997, ApJ, 478, 13
Steinmetz M., Muller E., 1995, MNRAS, 276, 549
Sugimoto D., Chikada Y., Makino J., Ito T., Ebisuzaki T., Umemura M., 1990, Nat, 345, 33
Thomas P.A. et al. , 1998, MNRAS, 296, 1061
van der Kruit P.C., 1987, A&A, 173, 59
Weil M.L., Eke V.R., Efstathiou G., 1998, MNRAS, 300, 773